

High strength and fatigue properties of Mg-Zn-Ca alloys after severe plastic deformation

E. V. Vasilev¹, V. I. Kopylov², M. L. Linderov¹, A.
I. Brilevsky¹, D. L. Merson¹, A. Yu. Vinogradov³

¹Institute of Advanced Technologies, Togliatti State University, 14 Belorusskay St., Togliatti, 445020, Russia

²Lobachevsky State University of Nizhni Novgorod, 23 Gagarin Av., Nizhniy Novgorod, 603950, Russia

³Department of Mechanical and Industrial Engineering, Norwegian University of Science and Technology, NTNU, Trondheim, N-7491, Norway

d.merson@tltsu.ru

Magnesium alloys are the lightest metallic structural materials with an outstanding specific strength. This makes them appealing for a wide range of applications in “green” transportation where weight saving is of major concern. Another emerging application area for modern Mg-based alloys is in the biomedical domain where they are considered as bioabsorbable temporary implants, and where the worldwide market is expanding particularly rapidly in parallel with the surging research. Requirements for mechanical properties — strength, ductility and fatigue resistance — of implants in orthopaedics are stringent. Therefore, a broad variety of processing routes have been proposed in the past decade to tailor the microstructure in order to optimize the properties. In the present brief communication, we demonstrate that using a hybrid deformation processing schedule involving warm equal-channel angular pressing (ECAP) on the first stage and cold rotary swaging on the second dramatically improves the tensile and fatigue properties of the magnesium alloy ZX40. Due to a combined effect of significant grain refinement and dislocation storage after rotary swaging, the ultimate tensile strength and the conventional fatigue limit achieved very high values (for this class of alloys) of 380 MPa and 115 MPa, respectively. Preliminary results of the microstructural investigations are discussed briefly.

Keywords: severe plastic deformation, magnesium alloys, mechanical properties, fatigue.

УДК: 538.951

Повышение прочностных и усталостных свойств Mg-Zn-Ca сплавов с помощью методов интенсивной пластической деформации

Васильев Е. В.¹, Копылов В. И.², Линдеров М. Л.¹, Брилевский А. И.¹,
Мерсон Д. Л.¹, Виноградов А. Ю.³

¹Научно-исследовательский институт прогрессивных технологий, Тольяттинский государственный университет, ул. Белорусская, 14, Тольятти, 445020, Россия

²Нижегородский государственный университет им. Н. И. Лобачевского, пр. Гагарина, 23, Нижний Новгород, 603950, Россия

³Факультет механики и промышленности, Норвежский технологический университет, Тронхейм, N-7491, Норвегия

Магниеые сплавы — это самые легкие металлические конструкционные материалы с уникально высокой удельной прочностью, что чрезвычайно перспективно для широкого спектра применений в «зеленом» транспорте, где снижение веса является первостепенной задачей. Другой новой областью применения современных сплавов на основе магния является биомедицина, в которой они позиционируются в качестве биорезорбируемых временных

имплантатов, и в которой мировой рынок расширяется особенно быстро, благодаря активации все больших объемов научно-исследовательских работ. Требования к механическим свойствам (прочности, пластичности и усталостной прочности) имплантатов в ортопедии являются очень высокими, поэтому в последнее десятилетие было предложено большое разнообразие способов обработки магниевых сплавов для адаптации микроструктуры с целью оптимизации их свойств. В настоящем кратком сообщении продемонстрировано, что использование гибридной схемы деформационной обработки, сочетающей теплое равноканальное угловое прессование на первой стадии и холодную ротационную ковку на второй, значительно улучшает свойства на растяжение и усталость магниевого сплава ZX40. Благодаря такой обработке за счет эффективного измельчения зерна и накопления дислокаций предел прочности при растяжении и предел усталости достигли очень высоких значений для этого класса сплавов: 380 МПа и 115 МПа соответственно. Кратко проанализированы результаты микроструктурных исследований.

Ключевые слова: интенсивная пластическая деформация, магниевые сплавы, механические свойства, усталость.

1. Introduction

In the search for efficient biodegradable materials for medical application a broad variety of alloy systems has been developed and investigated. Substantial attention has been paid to simple binary Mg-Zn, Mg-Ca and ternary Mg-Zn-Ca biocompatible systems [1]. An excellent combination of mechanical and corrosion properties has been demonstrated for the high purity extruded Mg-Zn-Ca ZX10 and ZX50 alloys [2,3] containing a specific noble intermetallic phase $Mg_6Zn_3Ca_2$. Besides many factors such as bio-compatibility, non-toxicity, bio-degradability, etc., the application of materials as temporary implants stipulates stringent requirements regarding integrity of implanted devices over the whole period of healing. This tacitly assumes that the mechanical properties remain sufficiently stable during a fairly long time while the implant is deployed is being gradually absorbed in the body. Fatigue and corrosion fatigue properties are of principal concern, to this end.

Improvement of high cycle fatigue (HCF) properties of structural materials is often based on the empiric correlation between the monotonic strength and the fatigue limit. This correlation follows straightforwardly from the Basquin law implying that the fatigue strength coefficient is related to the ultimate tensile strength σ_{UTS} under monotonic loading, and that the higher the σ_{UTS} value, the longer the HCF life and the higher the endurance limit under fully reversible loading. This correlation generally holds for steels, but it is also valid for light commercial alloys (based on Al and Ti) [4,5] [6,7] and Mg-alloys [8]. Thus, the increasing monotonic strength has been proven efficient for improving the HCF performance of many structural materials even through the higher σ_{UTS} does not guarantee the longer HCF life, e.g., for example, in non-heat treatable Al-alloys [9]. The yield stress and the ultimate tensile strength of the materials can be improved dramatically in the course of severe plastic deformation (SPD) due to a combination of influencing factors — Hall-Petch hardening, dislocation accumulation, which occur concomitantly with texture strengthening and refinement and redistribution of strengthening phases [10]. There have been many SPD techniques developed for different purposes in the past decades. For example, equal channel angular pressing (ECAP) emphasising simple shear deformation mode in a working billet results in substantially improved strength and sacrificed ductility of

many structural alloys [11], while magnesium under the same processing exhibits a compromised strength but a notable increased ductility [12]. A beneficial combination of properties can be often achieved through a combination of different processing routes. For example, by combining warm (or hot) ECAP and cold working, the residual ductility after ECAP can be “converted” into strength via further grain refinement and/or dislocation hardening [13]. Particularly, for deformation processing of rods, rotary swaging (RS) [14] is a well-received technique, which has been proven effective for grain refinement and strength improvement of Mg and its AZ31 alloy [15,16].

In the present brief communication, we endeavour to demonstrate that employing a hybrid two-step processing scheme involving warm equal-channel angular pressing (ECAP) followed by cold rotary swaging of ZX40 Mg-Zn-Ca alloy yields an outstanding combination of very high strength and excellent fatigue resistance.

2. Experimental

Ingots of commercial purity ZX40 series Mg-Zn-Ca gravity cast alloys with the nominal composition Mg-4Zn-0.1Ca (in wt.%) were annealed at 350°C for 24 h and subjected to two isothermal ECAP passes through the 90° rectangular die with sharp corners. ECAP was performed via Route B_C at 350°C. Part of the ECAP processed billets of 14×14 mm² cross-section was machined to cylindrical rods of 14.3 mm diameter which were then two-pass rotary swaged with the extrusion ratio 1.55 at room temperature.

Microstructural observations were carried out using a scanning electron microscope (SEM) Zeiss SIGMA equipped with the field emission gun, the EDAX/TSL electron back scattered diffraction (EBSD) detector and the orientation image microscopy software package.

The specimens for mechanical testing were cut by spark erosion along the extrusion direction. Uniaxial tensile tests were conducted on I-shaped specimens with the 10×4×3 mm² using the screw-driven testing machine under constant strain rate of 1×10⁻⁴ s⁻¹. For the fatigue tests, the sub-size hourglass specimens with the minimum cross-section of 2×2 mm² were used. Prior to mechanical testing or microstructural analysis, the samples were mechanically and electrolytically polished to a mirror like finish. An Instron Electropuls E1000 electro-mechanical testing machine was used for symmetric push-pull testing at ambient temperature in air at constant stress amplitude at 10 Hz frequency.

3. Results and Discussion

The microstructure of the as-cast alloy ZX40 is typical of that in Mg-Zn-Ca alloys with relatively small content of Ca (see, for example, [17] for Mg-3Zn- x Ca with x between 0 and 1.3 wt.%, [18] for Mg- x Zn-(0.8–1)Ca with different Zn content from 0 to 6 wt.% [19]). The as-cast alloy consists of almost equiaxed grains with average size of 220 μm . The coarse $\text{Ca}_2\text{Mg}_6\text{Zn}_3$ intermetallic phase is distributed unevenly as a continual network around grain boundaries and in the grain interior as described in [20]. The X-ray diffraction analysis shows that the Mg_2Ca phase is not present in the present alloy. The formation of Mg_2Ca phase in Mg-Zn-Ca alloys depends on the Zn/Ca atomic ratio. When this ratio is greater than 1.23, like it is in our case, the Mg_2Ca phase does not form [21]. Fig. 1 shows the orientation maps of the materials cross-section parallel to the extrusion direction (ED) after ECAP and ECAP+RS processes. Warm ECAP resulted in considerable refinement of the as-cast microstructure. The grain size reduced from 220 μm to about 20–30 μm . The microstructure after ECAP consisted predominantly of nearly uniform, fine, equiaxed recrystallized grains. The grain size distribution after ECAP is wide, being indicative of a relatively inhomogeneous microstructure, containing a mixture of large and small grains with the average size of 27.5 μm . It importantly to notice that despite the high homologous deformation temperature, the mechanical twins, primarily of the $\{10\text{--}12\}\langle 10\text{--}11\rangle$ extension type, are abundantly present in the microstructure. This opposes to plausible expectations that high temperature deformation suppresses twinning due to activation of non-basal dislocation slip modes. Since the twin lamellae have been systematically observed in the investigated ECAPed specimens, it might be supposed that the non-basal slip mode in Mg-alloys is not efficient enough to accommodate the strongly localised the simple shear deformation confined to a narrow zone along the plane of intersection between the channels (shear plane). Rotary swaging at room temperature results in further significant grain refinement. The average grain size reduced to $\sim 10\ \mu\text{m}$ though the heterogeneity of the microstructure remained or even increased due to very fine sub-microcrystalline grains coexisting with the original coarse grains (cf. Fig. 1a,b; notice the difference in the scale). The shear deformation bands formed during rotary swaging and intersecting at right angle are decorated by newly nucleated very fine grains of micrometre and sub-micrometre size. A large number of deformation twins is evident from the IPF map of the ECAPed specimen, Fig. 1a, while the population of twins is obviously reduced after rotary swaging due to significant grain refinement.

Fig. 2 shows the tensile stress-strain diagrams for the ECAP– and ECAP+RS processed samples. In line with expectations and common observations [12], the excellent strain hardening capacity and tensile ductility are gained in warm ECAPed Mg alloys primarily due to the texture effects. After post-ECAP RS processing the conventional yield stress $\sigma_{0.2}$ increased from 71 ± 4 to 127 ± 3 MPa, and the ultimate tensile strength, which was of 245 ± 8 MPa after 2 ECAP passes, exceeded 380 MPa (381 ± 5 MPa), which is notably high for

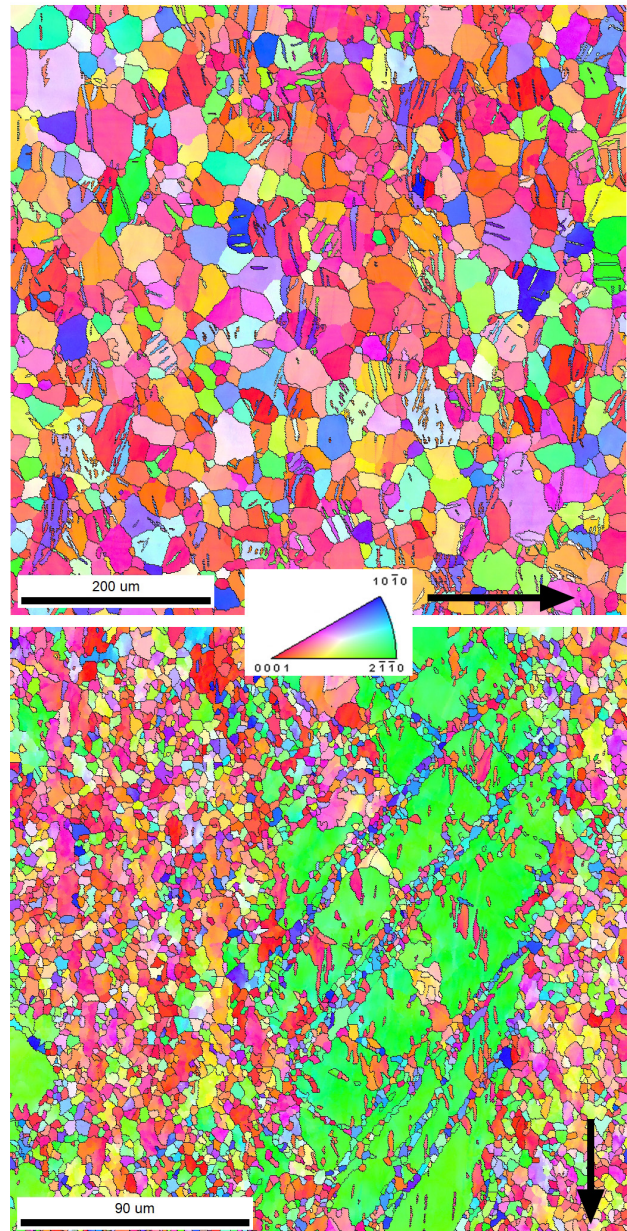


Fig. 1. (Color online) Orientation maps of the material's cross-section normal to the extrusion direction after ECAP and ECAP+SW processes. The color code corresponds to the inverse pole figure IPF (shown in the inset). Arrows indicate the extrusion direction.

Mg-Zn-Ca alloys (cf. also data reported in [20] for the same Mg-4Zn-0.1Ca alloy and the alloy Mg-4Zn-0.56Ca processed by ECAP under different conditions; a strong influence of processing parameters on the resultant mechanical response can be noticed). A trade-off between the tensile strength and ductility, which is commonly seen in the majority of SPD manufactured metals and alloys [10,11], is however evident. Due to a combined effect grain size reduction, dislocation accumulation and texture transformation, the yield stress and the ultimate tensile strength increase to the values which have never been reported so far for this class of nominally low strength alloys, to our best knowledge. Concurrently, in line with common expectations, the elongation to failure reduces albeit not to a prohibitively low level.

Wöhler S-N diagrams are shown in Fig. 3. Reference data for the extruded alloys WE43 (Mg-Y-RE) [22], ZX20 [23]

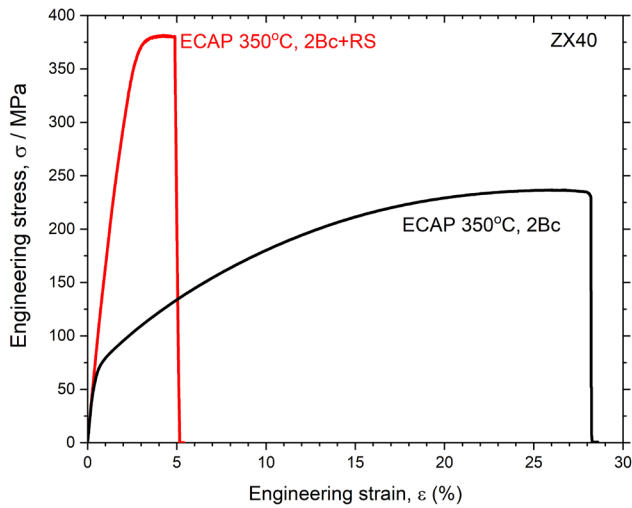


Fig. 2. Tensile stress-curves of ECAPed and ECAP+RS processed ZX40 alloy.

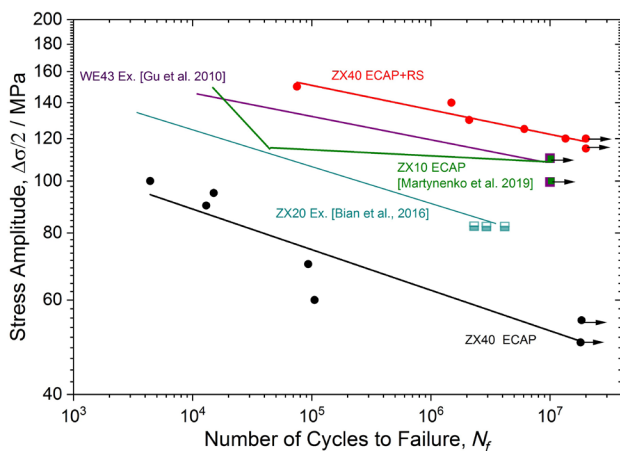


Fig. 3. (Color online) S-N plots for ECAPed and ECAP + RS processed ZX40 alloy (literature data are plotted for comparison by solid lines and symbols corresponding to fatigue life close to the fatigue limit; here “Ex.” abbreviates “Extrusion”).

and ZX10 [24] (Mg-Zn-Ca) are also shown by solid lines fitting experimental data for comparison. Fatigue properties of the ZX40 alloy after ECAP are modest as is often observed for many wrought Mg-based alloys [25]. However, the high cycle fatigue life of the rotary swaged samples is improved remarkably and the fatigue limit increased up to 125 MPa at 10^7 cycles, i.e. the endurance limit increased by a factor of two or more compared to its ECAPed counterpart. Importantly is that it is also notably higher than the fatigue limit values σ_{-1} reported for the symmetrically push-pull testing of the conventionally extruded WE43, ZX20 and ZX10 alloys, which are commonly considered as potent candidates for biomedical applications. Recent results reported in [24] for the fine grain Mg-1Zn-0.3Ca alloy after multipass (10 B_c passes were performed through the 120° die with the stepwise decreasing deformation temperature from 400 to 300°C) ECAP are remarkably good: $\sigma_{0.2} = 106 \pm 7$, $\sigma_{\text{UTS}} = 215 \pm 9$ MPa and $\sigma_{-1} = 110$ MPa. Although the ultimate strength, endurance limit and the elongation at break were slightly smaller than in the present paper for the alloy ZX40, the fatigue ratio $\sigma_{-1}/\sigma_{\text{UTS}} = 0.51$ was exceptionally high; cf. in the present work $\sigma_{-1}/\sigma_{\text{UTS}} = 0.22$ for the ECAPed samples and

0.33 for the samples after the hybrid ECAP + RS processing. The favourable comparison of the HCF life achieved in the studied ZX40 alloys with that in the alloy WE43 is particularly noteworthy. The alloy WE43 is a relatively heavily alloyed system with a large content of RE elements. With $\sigma_{0.2}$ and σ_{UTS} frequently reported to be in the range of 180 – 290 MPa and 280 – 330 MPa, respectively, this alloy admittedly belongs to a class of high strength alloys. Besides, it has been already deployed in biomedical applications. Furthermore, the fatigue strength exhibited by the fine-grained ZX40 alloy at the level of 120 – 125 MPa is comparable or even superior not only to many commercial Mg alloys, but also to many wrought Al alloys widely accepted in engineering practice [4].

Undoubtedly, the mechanical behaviour of magnesium alloys depends strongly, besides grain size, on texture [26]. The texture development in Mg alloys has been extensively studied for various processing routes including forging, extrusion, ECAP [12,27] and swaging [15,16]. For the route B_c , ECAP deformation gives rise to the basal fibre, which develops at about the 45° to ED [27,28]. Our observations align perfectly with those early findings. The materials flow during further swaging deformation resembles that during multiple axial forging and extrusion of a working billet [16]. Finally, the strong basal fibre texture forms with the basal planes parallel to the extrusion direction which is again in good agreement with the detailed texture analysis performed for RS-processed magnesium alloys [15,16]. Since the present brief communication is focused on the superior mechanical properties of the hybrid-processed ZX40 alloy, and the microstructure is only superficially described here, the detailed results of texture investigations and transmission electron microscopy observations will be reported elsewhere.

4. Conclusions

The nominally low strength Mg-Zn-Ca alloys with the fine grain microstructure obtained by hybrid SPD processing comprising of high temperature ECAP and room temperature rotary swaging demonstrated extraordinary, for this class of biodegradable alloys, tensile and fatigue strength and moderate ductility. This combination appears promising for a wide range of applications of these light weight biocompatible and biodegradable alloys.

Acknowledgements. This work was supported by the Ministry of Science of RF under grant-in-aid RFMEFI58317X0070.

References

1. B. P. Zhang, Y. Wang, L. Geng. Research on Mg-Zn-Ca Alloy as Degradable Biomaterial, *Biomaterials — Physics and Chemistry*. In: R. Pignatello (Ed.). *Biomaterials*, InTech (2011) [Crossref](#)
2. J. Hofstetter, M. Becker, E. Martinelli, A. M. Weinberg, B. Mingler, H. Kilian, S. Pogatscher, P. J. Uggowitzer, J. F. Löffler. *JOM*. 66 (4), 566 (2014). [Crossref](#)
3. J. Hofstetter, E. Martinelli, S. Pogatscher, P. Schmutz, E. Povoden-Karadeniz, A. M. Weinberg, P. J. Uggowitzer, J. F. Löffler. *Acta Biomaterialia*. 23, 347 (2015). [Crossref](#)

4. Y. Estrin, A. Vinogradov. *International Journal of Fatigue*. 32(6), 898 (2010). [Crossref](#)
5. A. Vinogradov, A. Washikita, K. Kitagawa, V. I. Kopylov. *Materials Science and Engineering A*. 349(1-2), 318 (2003). [Crossref](#)
6. L. R. Saitova, H. W. Höppel, M. Göken, I. P. Semenova, R. Z. Valiev. *International Journal of Fatigue*. 31(2), 322 (2009). [Crossref](#)
7. A. Y. Vinogradov, V. V. Stolyarov, S. Hashimoto, R. Z. Valiev. *Materials Science and Engineering A*. 318 (1-2) 163 (2001).
8. R. B. Heywood, *Designing against fatigue of metals*. Reinhold, New York (1962) 436 p.
9. V. Patlan, A. Vinogradov, K. Higashi, K. Kitagawa. *Materials Science and Engineering A*. 300(1-2), 171 (2001). [Crossref](#)
10. Y. Estrin, A. Vinogradov. *Acta Materialia*. 61(3), 782 (2013). [Crossref](#)
11. A. Vinogradov. *Advanced Engineering Materials*. 17(12), 1710 (2015). [Crossref](#)
12. S. R. Agnew, J. A. Horton, T. M. Lillo, D. W. Brown. *Scripta Materialia*. 50(3), 377 (2004). [Crossref](#)
13. I. P. Semenova, G. K. Salimgareeva, V. V. Latysh, R. Z. Valiev. *Solid State Phenomena*. 140, 167 (2008). [Crossref](#)
14. M. Wang, Y. Wang, A. Huang, L. Gao, Y. Li, C. Huang. *Materials*. 11(11), 2261 (2018). [Crossref](#)
15. J. Muller, M. Janecek, L. Wagner. *Materials Science Forum*. 584 – 586, 858 (2008). [Crossref](#)
16. W. M. Gan, Y. D. Huang, R. Wang, G. F. Wang, A. Srinivasan, H. G. Brokmeier, N. Schell, K. U. Kainer, N. Hort. *Materials & Design*. 63, 83 (2014). [Crossref](#)
17. K. Kubok, L. Lityńska-Dobrzyńska, J. Wojewoda-Budka, A. Góral, A. Dębski. *Archives of Metallurgy and Materials*. 58(2), 329 (2013). [Crossref](#)
18. H. R. Bakhsheshi-Rad, E. Hamzah, A. Fereidouni-Lotfabadi, M. Daroonparvar, M. A. M. Yajid, M. Mezbahul-Islam, M. Kasiri-Asgarani, M. Medraj. *Materials and Corrosion*. 65(12), 1178 (2014). [Crossref](#)
19. B. Zhang, Y. Hou, X. Wang, Y. Wang, L. Geng. *Materials Science and Engineering: C*. 31(8), 1667 (2011). [Crossref](#)
20. A. Vinogradov, E. Vasilev, M. Linderov, D. Merson. *Metals*. 6(12), 304 (2016). [Crossref](#)
21. H. R. Bakhsheshi-Rad, M. R. Abdul-Kadir, M. H. Idris, S. Farahany. *Corrosion Science*. 64, 184 (2012). [Crossref](#)
22. X. N. Gu, W. R. Zhou, Y. F. Zheng, Y. Cheng, S. C. Wei, S. P. Zhong, T. F. Xi, L. J. Chen. *Acta Biomaterialia*. 6(12), 4605 (2010). [Crossref](#)
23. D. Bian, W. Zhou, Y. Liu, N. Li, Y. Zheng, Z. Sun. *Acta Biomaterialia*. 41, 351 (2016). [Crossref](#)
24. N. Martynenko, E. Lukyanova, V. Serebryany, D. Prosvirnin, V. Terentiev, G. Raab, S. Dobatkin, Y. Estrin. *Materials Letters*. 238, 218 (2019). [Crossref](#)
25. V. V. Ogarevic, R. I. Stephens. *Annual Review of Materials Science*. 20(1), 141 (1990). [Crossref](#)
26. S. Biswas, S. S. Dhinwal, S. Suwas. *Acta Materialia*. 58(9), 3247 (2010). [Crossref](#)
27. B. Beausir, S. Suwas, L. S. Tóth, K. W. Neale, J. J. Fundenberger. *Acta Materialia*. 56(2), 200 (2008). [Crossref](#)
28. V. N. Serebryany, T. M. Ivanova, T. I. Savyolova, S. V. Dobatkin. *Solid State Phenomena*. 160, 159 (2010). [Crossref](#)